# Quantum-Mechanical Continuum Solvation Study of the Polarizability of Halides at the Water/Air Interface

**Luca Frediani,[†] Benedetta Mennucci,*[,‡] and Roberto Cammi[†]**

*Dipartimento di Chimica, Università di Parma, Viale delle Scienze 17/A, 43100 Parma, Italy, and Dipartimento di Chimica, Università di Pisa, Via Risorgimento 35, 56126 Pisa, Italy*

*Received: April 10, 2004; In Final Form: July 8, 2004*

In this work, a theoretical study of static polarizabilities of halides (fluoride, chloride, bromide and iodide) at the water/air interface is presented. The study has been carried out employing a new development of the polarizable continuum model (PCM) to treat model interfaces between two different media. Within this framework the water/air interface is modeled as a water/vacuum interface having bulk properties (e.g., density or permittivity) varying smoothly from the bulk water to the vacuum in the interfacial region. The model allows the inclusion of electrostatic and repulsion effects arising from this inhomogeneous environment into the quantum chemical calculation for each of the selected ionic species. Static polarizabilities are then calculated as a function of the ion−interface distance. The results on polarizabilities together with those obtained for other properties and with free energy profiles are finally discussed in relation to the recent simulation results showing a preference of heavier halides for the interface than for bulk water.

## 1. Introduction

Solvation of halogen anions at the liquid/air interface is an important aspect in many environmental and atmospheric problems, and many theoretical and experimental studies have been performed, especially in the last years. On the experimental side, no direct proof of surface solvation is available, but indirect evidence exists involving the uptake of halogens by halide solutions.[1] This has been interpreted by postulating a surfactant behavior of halide anions, i.e., their preference to be located at the interface rather than in the bulk solution.

The lack of direct investigations concerning these challenging systems in connection with their importance has triggered a sizable amount of theoretical work on the subject.

The first attempt to study ion solvation at interfaces has been based on the classical Onsager theory of electrolytes.[2,3] In this approach, interfaces were naively represented as boundaries dividing different regions of physical space and ions as nonpolarizable point charges. According to this classical electrostatics model, ion concentration diminishes while approaching the interfacial region and it becomes null at the interface. This result contrasts with what is suggested by the experiments. Thus it appears evident that modelization of interfaces cannot be given in terms of simple boundaries, and ions require a more accurate representation than a point charge description.

In the last years, the theoretical modeling of the interfaces has received renewed attention, as demonstrated by the recently published review by Jungwirth and Tobias,[4] to which we refer for the literature on the subject. Following their presentation we can identify three main steps in the theoretical modeling of these systems. The first step involved classical molecular dynamics (MD) simulations of halide solution/vacuum interfaces with nonpolarizable force fields, which showed a diminished ion concentration at the surface as in the classical Onsager model. In a second step, accurate ab initio calculations on small ion/water clusters were performed, giving the first theoretical evidence of heavier halides' ($Cl^-$, $Br^-$, $I^-$) preference for the interfacial environment. In the third step, MD simulations were performed using many-body polarizable potentials, which confirmed the ab initio assessment of interfacial preference of heavier halides. On the basis of the evolution of these theoretical studies it has been concluded that the polarizability of the ion plays a crucial role in inducing a surfactant behavior of heavier halides.

Due to this fundamental role, attention has been devoted to the determination of the polarizability in vacuo, in solution, and for interfacial environments. From the theoretical point of view, the determination of the polarizability of solvated systems is more complex. One can in fact obtain the polarizability of the whole system (solute + solvent), but it is not straightforward to extract each single contribution since the molecular polarizability is not an additive property. In parallel, it is not easy to determine how the polarizability of a molecule is affected by the surrounding environment.[5]

Three main alternative approaches have been proposed:

(i) modeling the solvent molecules as classical nonpolarizable point charges, thus not contributing to the solute polarizability;

(ii) using a "supermolecule" approach and subtracting the property of the solvation shell from that of the solvated cluster (solute + solvation shell);

(iii) using a solvation continuum method and computing the property of the solute perturbed by the continuum solvent.

The first approach is simple and cost-effective, but it has the limit of neglecting solute−solvent polarization effects. The second one yields a good description of the solute−solvent interactions, but it has the weak point of imposing additivity in the property, and this can be considered reasonable only for weakly interacting systems, but not for anion−water systems. The last approach combines the advantage of taking into account mutual solute−solvent polarization effects with a treatment that

* Corresponding author. E-mail: bene@dcci.unipi.it.
[†] Università di Parma.
[‡] Università di Pisa.

10.1021/jp048414s CCC: $27.50 
Published on Web 08/17/2004

is formally equivalent to the isolated system. Obviously, also this approach presents limits, among which the most important one is the lack of a microscopic description of the solvent molecules, which prevents properly accounting for specific solute−solvent interactions.

While the first two models have already been applied to the study of molecular polarizability of ions both in bulk and at interfaces, the continuum approach has seldom been employed to study the polarizability of ions, whereas for neutral species it has been widely used.[6] In this work we present a theoretical study of halide ions at the interfaces based on the polarizable continuum model (PCM).[7,8] The present application has been made possible by a recent extension of the PCM to diffuse interfaces,[9,10] which offers the possibility to treat the solution, interfacial environment, and the isolated system with a single computationally and physically coherent scheme.

In section 2 we will review the solvation model with particular emphasis on those aspects which have been developed for the present study. In section 3 we will discuss the choice of the level of calculation (method and basis set) used for the interface calculations and we will show and discuss the obtained results for the four halides at the water/vacuum interface; when possible we will compare our findings with results obtained in previous works.

## 2. Theory

In this section, we present the theoretical apparatus needed to study polarizability profiles of molecules from the bulk solution to the vacuum phase passing through the diffuse interface. These systems will be treated by modeling the environment surrounding the molecule as a dielectric medium characterized by a dielectric permittivity and a density continuously varying along the direction perpendicular to the interface (here $z$) and constant on the plane (here along $x$ and $y$ directions). Such a model is an extension of the integral equation formalism (IEF)[11−13] version of the PCM.

**2.1. Electrostatic Model.** In the basic formulation of the model, which includes only the electrostatic part of the solute−solvent interaction, the system can be represented as a quantum mechanical charge distribution $\rho(\boldsymbol{r})$ hosted in a cavity $C$ inside a continuum medium having a dielectric constant $\epsilon$:

$$\begin{cases} L_i V(\boldsymbol{r}) = -4\pi\rho(\boldsymbol{r}) & \forall \boldsymbol{r} \in C \\ L_e V(\boldsymbol{r}) = 0 & \forall\, \boldsymbol{r} \notin C \end{cases} \tag{1}$$

where we have formulated the problem in terms of Poisson's equation inside and outside the cavity. In eq 1 $L_i = \nabla^2$ is the Laplacian operator; $L_e = \nabla\cdot\epsilon(\boldsymbol{r})\nabla$ is the correct operator to be used for a dielectric medium of permittivity $\epsilon(\boldsymbol{r})$. When the permittivity is a constant, this operator is reduced to the more common form $\epsilon\nabla^2$.

Within the PCM framework, the solution of the electrostatic problem (eq 1) is obtained by introducing an apparent surface charge (ASC) $\sigma(\boldsymbol{s})$ placed on the cavity boundary $\Gamma_C$. To evaluate $\sigma(\boldsymbol{s})$, the numerical procedure called boundary element method (BEM) is used. Namely it consists of dividing the cavity surface into $N$ small patches (or tesserae): for each tessera, the area $a_i$ is calculated, a representative point $\boldsymbol{s_i}$ is selected, and the apparent surface charge $\sigma(\boldsymbol{s})$ is approximated with a set of point charges collected in a vector $\boldsymbol{q}$. Each element of this vector is defined as $q_i = \sigma(\boldsymbol{s_i})\cdot a_i$. In this way, the electrostatic problem can be reformulated in a matrix form:[13]

$$\boldsymbol{q} = \boldsymbol{Q}\boldsymbol{V} \tag{2}$$

where $\boldsymbol{V}$ is the electrostatic potential produced by the density $\rho$ on the selected set of cavity points and $\boldsymbol{Q}$ is an appropriate square matrix whose construction depends on the version of PCM that is adopted.

In the framework of IEF-PCM, the most important quantity required to obtain the matrix $\boldsymbol{Q}$ of eq 2 is Green's function $G(\boldsymbol{x},\boldsymbol{y})$ of the problem under investigation. Green's function of an electrostatic problem is the potential produced in $\boldsymbol{y}$ by a unit point charge located in $\boldsymbol{x}$. For instance, for a homogeneous and uniform dielectric, Green's function outside (external) the cavity is $G_E(\boldsymbol{x},\boldsymbol{y}) = 1/(\epsilon|x - y|)$, which, by the above definition, is the solution of the following equation:

$$\nabla_{\mathbf{r}}[\epsilon(\boldsymbol{r})\cdot\nabla_{\mathbf{r}} G_E(\boldsymbol{r},\boldsymbol{r}')] = -4\pi\delta(\boldsymbol{r} - \boldsymbol{r}') \tag{3}$$

By knowing the Green's functions outside and inside the cavity, it is possible to solve a system formally equivalent to the set of equations (1) and thus to define the proper apparent charges. Besides the homogeneous and uniform dielectric, there are other physical environments that have been treated within such an approach: they are modeled by varying the form of the operator $L_e$ to properly describe the selected physical system. In particular there are analytical solutions for liquid crystals, ionic solutions,[11,12] sharp planar interfaces between two dielectrics,[9] and liquid/metal interfaces.[14,15]

More recently Frediani et al.[10] have developed a formulation that generalizes the IEF-PCM theory to a system with a position-dependent dielectric constant, which can be described with an $\epsilon(\boldsymbol{r})$ function. To study planar diffuse interfaces, the authors have assumed an $\epsilon(\boldsymbol{r})$, varying along the $z$ axis and isotropic. Formally, Green's function can now be obtained by replacing the dielectric constant $\epsilon$ in eq 3 with the chosen permittivity profile $\epsilon(z)$. This equation is no longer solvable analytically for a general permittivity profile, but a numerical integration is required for each couple of points $\boldsymbol{r}$ and $\boldsymbol{r}'$.

The interested reader can find the details of the derivation in the original paper;[10] here we report only the final expression:

$$G_E(\vec{r},\vec{r}') = \frac{1}{D(\epsilon(z))|\vec{r} - \vec{r}'|} + G_E^{\mathrm{img}}(\vec{r},\vec{r}') \tag{4}$$

where the first term is a Coulomb-like term having the same form of Green's function for a homogeneous dielectric environment but with the dielectric constant $\epsilon$ replaced by the term $D$, which depends on the permittivity profile of the interface. The second term is the image potential of a sharp interface, which is treated separately in order to overcome the divergence it would cause in the numerical integration.

**2.2. Permittivity Profile at the Interface.** Due to the flexibility of the procedure used to evaluate the electrostatic Green's function, any continuous profile for the permittivity $\epsilon(\boldsymbol{r})$, with a not too large derivative and that does not cross the zero, can be considered. The choice of the dielectric profile thus depends on which system we want to mimic.

Although determinations of dielectric permittivity profiles of interfaces are lacking, different studies on solvent density profiles $\rho(z)$ at liquid/gas and liquid/liquid interfaces have been published.[16,17] For instance, liquid/gas profiles are usually fitted with a function of the form

$$\rho(z) = \frac{\rho_B}{2}\left[1 \pm \tanh\left(\frac{z - z_0}{D}\right)\right] \tag{5}$$

where $\rho_B$ is the bulk density and the sign $\pm$ depends on which region of space ($z > z_0$ or $z < z_0$) is occupied by the liquid. $D$

in eq 5 is an adjustable parameter that defines the width of the interface. Following the analysis reported in ref 10, here we have used a value of $D$ that corresponds to a thickness (defined as the region of space across the interface where the density varies from $0.1\rho_B$ to $0.9\rho_B$) of 2.56 Å (or $W = 7$ Å to keep the notation used in the reference paper). This value has been determined to obtain agreement with the density profiles obtained through molecular dynamics simulations.[18−20]

The density profile of eq 5 represents here the starting point to define the permittivity profile. By assuming a linear relation between the permittivity and the density, and by taking into account proper boundary conditions, for a planar interface between a liquid and vacuum we obtain[10]

$$\epsilon(z) = \frac{\epsilon_B + 1}{2} \pm \frac{\epsilon_B - 1}{2}\tanh\left(\frac{z - z_0}{D}\right) \qquad (6)$$

where $\epsilon_B$ is the bulk permittivity of the liquid. Far from $z_0$, this function is almost constant and equal to either the liquid permittivity $\epsilon_B$ or 1. In the interface region, the permittivity changes smoothly between these two values.

It is evident that the assumptions based on eq 6 neglect the effects of the interface on the orientational polarization of the water molecules. These effects introduce an anisotropy in the solvent response that makes the permittivity profile more complex than the one expressed by eq 6. A more detailed analysis of the validity and the limits of eq 6 can be found in ref 10.

**2.3. Quantum Mechanical Equations.** To insert the solute−solvent interactions into an ab initio calculation, it is necessary to define the effective Hamiltonian operator that represents the in vacuo Hamiltonian plus a solute−solvent interaction potential. For the moment we limit ourselves to the electrostatic interaction that is the most relevant one. In the next section an additional contribution referring to solute−solvent repulsion interactions will be introduced.

In the electrostatic approximation the solvent operator $\hat{V}_\Psi$ is expressed as a scalar product of a vector collecting the electrostatic potential onto the surface representative points, $\boldsymbol{V}$, by a vector containing the apparent point charges $\boldsymbol{q}$. The potentials $\boldsymbol{V}$, and consequently the charges $\boldsymbol{q}$, can be split into two terms, one due to the solute nuclei and the other due to the solute electrons. Following this subdivision of the solute charge density into electronic ($e$) and nuclear terms ($N$), it is possible to partition the operator $\hat{V}_\Psi$ accordingly by introducing operators of the general form

$$\hat{M}(x, y) = \sum_\tau \hat{V}_\tau^y \cdot q_\tau^x \qquad (7)$$

where $y$, $x$ can be $e$ or $N$. It is important to note that the operator corresponding to $x = y = e$, usually indicated as $\hat{X}_{el}$, is formally a bielectronic operator, but it is obtained as a product of two monoelectronic parts. Moreover, we have $\hat{M}(e,N) = \hat{M}(N,e) = \hat{h}_{el}$.

By applying a variational principle on the free energy functional $\mathcal{G}(\Psi)$ of the system, which is defined as

$$\mathcal{G}(\Psi) = \langle\Psi|\hat{G}_\Psi|\Psi\rangle = \left\langle\Psi\middle|\hat{H}_0 + \frac{1}{2}\hat{V}_\Psi\middle|\Psi\right\rangle \qquad (8)$$

and by introducing an expansion of the molecular orbitals in terms of a finite basis set, we obtain the appropriate Fock eigenvalue equation in which the Fock operator $\boldsymbol{F}'$ is defined as

$$\boldsymbol{F}' = \boldsymbol{h}' + \boldsymbol{G}'(\boldsymbol{P}) = \boldsymbol{h} + \boldsymbol{h}_{el} + \boldsymbol{G}(\boldsymbol{P}) + \boldsymbol{X}_{el}(\boldsymbol{P}) \qquad (9)$$

where $\boldsymbol{P}$ is the density matrix, $\boldsymbol{h}$ and $\boldsymbol{G}$ are the matrices corresponding to the in vacuo mono- and bielectronic operators, and $\boldsymbol{h}_{el}$ and $\boldsymbol{X}_{el}$ are the solvent-induced equivalents.

Until now we have considered solute−solvent electrostatic interactions only; in the following section we show how the same model can be extended to treat solute−solvent repulsion effects.

**2.4. Repulsion Energy: Extension to the Interface.** Following Amovilli and Mennucci,[21] the Pauli repulsion contribution to the solvation free energy can be written as

$$G_{rep} = \alpha\int_{\boldsymbol{r}\notin C} d\boldsymbol{r}\, P_A(\boldsymbol{r}) = \alpha[\int d\boldsymbol{r}\, P_A(\boldsymbol{r}) - \int_{\boldsymbol{r}\in C} d\boldsymbol{r}\, P_A(\boldsymbol{r})] \qquad (10)$$

with

$$\alpha = 0.063\rho_B\frac{n_{val}^B}{M_B} \qquad (11)$$

Here the label $A$ refers to the solute, $B$ refers to the solvent, $\rho_B$ is the density of the solvent relative to the density of water at 298 K, and $n_{val}^B$ and $M_B$ are the number of valence electrons and the molecular weight of the solvent.

Equation 10 shows a proportionality between the repulsion and the part of the solute electrons outside the cavity. This fraction of the electronic charge is given by the difference of total solute electronic charge and the electronic charge inside the cavity. By applying the Gauss theorem we obtain that the internal charge is $(1/4\pi)\int_\Gamma \vec{E}^A(\boldsymbol{r})\cdot\hat{n}_r\, d\boldsymbol{r}$ where $\hat{n}_r$ is the outward unit vector perpendicular to the cavity surface at point $\boldsymbol{r}$ and $\vec{E}^A$ the solute electric field due to the electrons only.

The repulsion free energy (eq 10) can be added to the electrostatic free energy defined in section 2.3 and the resulting quantity used in a variational way to get a new Schroedinger equation including also the repulsion term. By following the same approach used above, in which we introduce an expansion over a finite basis set $\{\chi\}$, eq 10 can be rewritten as follows:

$$G_{rep} = \alpha\, tr\, \boldsymbol{P}[\boldsymbol{S} - \boldsymbol{S}^{(in)}] = tr\, \boldsymbol{P}\boldsymbol{h}_{rep} \qquad (12)$$

where $\boldsymbol{S}$ is the orbital overlap matrix and

$$S_{\mu\nu}^{(in)} = -\frac{1}{4\pi}\int_\Gamma E_{\mu\nu}(\boldsymbol{r})\, d\boldsymbol{r} \qquad (13)$$

In this last expression $E_{\mu\nu}(\boldsymbol{r})$ is the normal component of the electric field integrals over the basis functions at the cavity surface. Equation 12 shows that repulsion interactions contribute to the Fock matrix of eq 9 only through a new one-electron matrix: $\boldsymbol{h}_{rep}$.

To derive eqs 10−13, we have assumed an isotropic and homogeneous solvent characterized by a constant density $\rho_B$. As a matter of fact, the same approach can be generalized to inhomogeneous system like the diffuse interfaces treated in section 2.2. This generalization leads to the following form for $G_{rep}$:

$$G_{rep} = \alpha'\int_{\boldsymbol{r}\notin C} d\boldsymbol{r}\, \rho(\boldsymbol{r})P_A(\boldsymbol{r}) \qquad (14)$$

where

$$\alpha' = 0.063\frac{n_{val}^B}{M_B} \qquad (15)$$

The numerical solution of the integral in eq 14 is very complex; we thus introduce an approximation by proposing the following:

$$G_{rep} = \alpha' \, tr \, \boldsymbol{P}[\bar{\rho}\boldsymbol{S} - \tilde{\boldsymbol{S}}^{(in)}] = tr\boldsymbol{P}\tilde{\boldsymbol{h}}_{rep} \tag{16}$$

where now

$$\tilde{S}^{(in)}_{\mu\nu} = -\frac{1}{4\pi}\int_{\Gamma}\rho(\boldsymbol{r})\, E_{\mu\nu}(\boldsymbol{r})\, d\boldsymbol{r} \tag{17}$$

Expressions 16 and 17 require some comments. The second contribution to $G_{rep}$, namely, that containing the dependence of the electric field on the cavity boundary, is now evaluated introducing the real position-dependent solvent density $\rho(\boldsymbol{r})$ inside the integral as a proper weight (see eq 17). On the other hand, the first contribution, namely, that containing the overlap matrix $\boldsymbol{S}$, is evaluated in an approximated way by introducing a density $\bar{\rho}$, which is averaged over the cavity boundary by means of the expression

$$\bar{\rho} = \frac{\int_{\Gamma}\rho(\boldsymbol{r})\, d\boldsymbol{r}}{\int_{\Gamma} d\boldsymbol{r}} \tag{18}$$

The resulting new repulsion matrix $\tilde{\boldsymbol{h}}_{rep}$ of eq 16 is thus an approximation to what should follow from a rigorous treatment of eq 14 but it still includes the main effects due to the solvent presenting a density continuously varying across the interface. We recall that all the integrals on the cavity surface are computed by exploiting the same BEM method used for the electrostatic terms, and thus they reduce to finite summations on the cavity tesserae.

**2.5. QM Calculation of Polarizabilities.** The theory of PCM for the calculation of the polarizabilities of molecular solutes is based on an ab initio variational-perturbative response scheme in the presence of an electric field.[22,23] The resulting Hamiltonian is

$$\hat{H} = \hat{H}_{eff} + \hat{\mu}[\mathbf{E}^{\omega}(e^{i\omega t} + e^{-i\omega t}) + \mathbf{E}^{0}] \tag{19}$$

where $\hat{H}_{eff}$ is the effective Hamiltonian including the solute−solvent interactions and $\hat{\mu}$ is the electronic dipole moment operator.

In eq 19, we have considered a general case of a time-dependent perturbation representing the interaction of the "solute" with the field formed by a static and an oscillating component. We note, however, that in the more specific case of static polarizabilities, i.e., the case studied in the present article, the oscillating component vanishes and the whole procedure reduces to a static perturbed scheme.

Approximate solutions of the time-dependent Schrödinger equation can be obtained by using the Frenkel variational principle. In the framework of a one-determinant wave function with orbital expansion over a finite atomic basis set, we arrive at the following time-dependent equation:

$$\mathbf{F}'\mathbf{C} - i\frac{\partial}{\partial t}\mathbf{S}\mathbf{C} = \mathbf{S}\mathbf{C}\epsilon \tag{20}$$

with the proper orthonormality condition; $\mathbf{S}$, $\mathbf{C}$, and $\epsilon$ represent the overlap, the MO coefficient, and the orbital energy matrices, respectively.

In eq 20 the prime on the Fock matrix indicates that terms accounting for the solvent effects are included, i.e.,

$$\mathbf{F}' = \mathbf{h} + \mathbf{G}(\mathbf{P}) + \mathbf{m}\cdot[\mathbf{E}^{\omega}(e^{i\omega t} + e^{-i\omega t}) + \mathbf{E}^{\circ}] + \tilde{\mathbf{h}}_{rep} + \mathbf{h}_{el} + \mathbf{X}_{el}(\mathbf{P}) \tag{21}$$

The solution of the time-dependent eq 20 can be obtained within a time-dependent coupled scheme by expanding all the involved matrices in powers of the field components. Limiting the analysis to the first-order, we obtain for the Fock operator (with $a$ indicating the Cartesian coordinate of the applied field)

$$\mathbf{F}'_{a} = \mathbf{G}(\mathbf{P}^{a}) + \mathbf{X}_{el}(\mathbf{P}^{a}) + \mathbf{m}_{a} \tag{22}$$

where we have eliminated the dependence on the frequency $\omega$ as here we are interested in the static case, and $\mathbf{P}^{a}$ is the perturbed density matrix at the first order.

By applying standard iterative procedures, the components of the static polarizability can be computed as

$$\alpha_{ab} = -tr[\mathbf{m}_{a}\mathbf{P}^{b}] \tag{23}$$

With this formalism it is possible to introduce the solvent effect both into the computation of the wave function and in its response to the applied external field. The resulting polarizability will thus be the combination of these two effects.

## 3. Numerical Results

**3.1. Quantum Mechanical Level and Bulk Solvation Model.** The accurate calculation of molecular polarizabilities is in general a difficult task, but here it is even more delicate, as we are considering anions. For anions in fact dynamical electron correlation accounts for a large fraction of their polarizability, and thus it is compulsory to exploit a correlated approach.

Another critical point in the calculation of polarizabilities for anions is the choice of the basis set. Already for the unperturbed anions a sufficient number of diffuse functions has to be considered to obtain an accurate description of its electronic structure. To calculate the polarizability of anions, the basis set must be augmented further with additional diffuse polarization functions with higher angular momenta. Here, to obtain reliable results, we use the large one-particle basis sets calibrated by Hattig and Hess[24] on the polarizabilities of anions by augmenting basis sets taken from the literature, with polarization functions of appropriate angular momenta and exponents. For the details about the construction and the calibration of these additional functions we refer to the reference paper;[24] here we only note that the starting basis set for such calibration is the correlation-consistent aug-cc-pV5Z basis of Woon and Dunning,[25] for F and Cl, and the well-tempered formula (WTF) basis from Huzinaga and Klobukowski,[26] for Br and I.

To evaluate the importance of the electronic description, we have used fluoride as the test system and exploited the HF method, DFT with the B3LYP functional, and MP2, which served as a benchmark. For each of the three selected methods, three basis sets have been used: the previously described basis set developed by Hattig and Hess (from now on referred to as the HH basis) and two standard basis sets, the aug-cc-pVDZ and the daug-cc-pVDZ basis sets. For each pair of method/basis set we have performed calculations in vacuo and in bulk solvent with the electrostatic model.

The data reported in Table 1 can be analyzed in different ways. Let us first focus on the behavior of the property in a given phase with respect to the QM calculation.

If we look at the gas-phase results, the importance of the dynamical correlation on the property appears evident: namely, B3LYP and MP2 results are quite similar while HF largely

**TABLE 1: Static Polarizabilities (au) of Fluoride in Gas and in Water (IEF-PCM) as a Function of the Calculation Method (HF, B3LYP, MP2) and the Basis Set (aug-cc-pVDZ, daug-ccpVDZ, HH)**

| | gas | | | IEF-PCM | | |
|---|---|---|---|---|---|---|
| | aug | daug | HH | aug | daug | HH |
| HF | 5.62 | 9.84 | 10.66 | 6.06 | 10.00 | 10.13 |
| B3LYP | 6.80 | 17.03 | 22.91 | 7.39 | 14.52 | 15.16 |
| MP2 | 6.77 | 14.53 | 16.85 | 7.28 | 13.79 | 14.33 |

underestimates the property. These findings give also an immediate confirmation that B3LYP can be used to obtain reliable results of the polarizability: it in fact represents a valid alternative to MP2, and thus it allows the use of very large bases also for those systems for which MP2 approach rapidly becomes unfeasible.

Passing now to the effect of the basis set, it is clear that the calibration made by Hess and Hattig leads to a quite different description with respect to the other two standard bases: limiting the comparison to the largest daug-cc-pVDZ, an increase of more than 8% is found for HF, more than 34% for B3LYP, and 16% for MP2. We also note that B3LYP presents the largest sensitivity with respect to the quality of the basis.

This analysis changes, at least in some aspects, when solvated fluoride is considered. A general feature of the IEF-PCM calculation is a reduced sensitivity to the basis set. This fact is explained considering that the effect of diffuse functions is largely reduced by the "squeezing action" of the dielectric continuum. Comparing the IEF-PCM results to their gas-phase counterparts, we can see that in solution the increase of the polarizability with the basis set is less steep than in the gas phase. As a consequence, the gas-to-solution shift of the polarizability is initially positive (i.e., in solution $\alpha$ is larger), but then it becomes negative with the largest HH basis set. We observe that, when correlation is introduced, this change of sign appears with the intermediate daug-cc-pVDZ.

*3.1.1. Continuum Model versus Discrete Approaches.* Here, we do not want to develop further the analysis of the effects of the QM level (and in particular of the combination method/basis set) on the gas-to-solution shift. We note, however, that the effects of solvation on the polarizability have been here computed in terms of an electrostatic-only continuum model, but other descriptions can be exploited. An obvious alternative with respect to a continuum model is represented by the "supermolecule" approach introduced in section 1. In this approach, the QM system is extended so to include not only the solute but also the solvent molecules in the first shell of solvation (or, more in general, those that directly and significantly interact with the solute). For an ion in water it is clear that strong H-bonding interactions apply between the ion and the water hydrogen atoms, and thus the ion plus the net of H-bonded water molecules immediately around it well represents the "supermolecule" system. Following the study by Jungwirth and Tobias,[27] we have considered the six closest waters arranged around the fluoride anion as represented in Figure 1.

The structure of this cluster has been obtained at the B3LYP/6-31++G(d) level: the H-bond distances are reported in Figure 1.

To evaluate the polarizability of fluoride in the cluster, we have to introduce a strong approximation, i.e., to assume that polarizability is additive and thus $\alpha(F^-)$ in the cluster can be obtained subtracting from $\alpha$(cluster) the polarizability of the 3D net formed by the six water molecules.

As reported in section 1, an alternative and computationally simpler method, which also avoids any assumption of additivity,

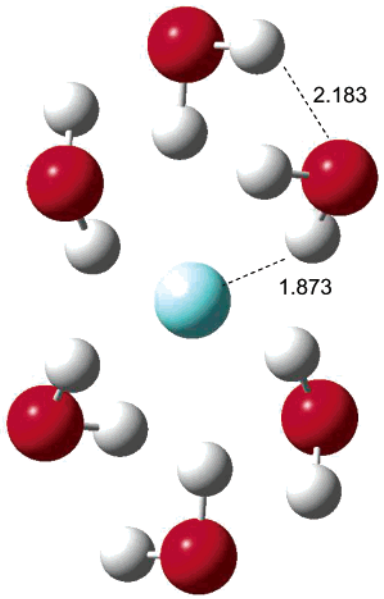


**Figure 1.** B3LYP/6-31++G(d) geometric structure of the $F(H_2O)_6^-$ cluster ($D_3$ symmetry). Reported distances are in Å.

**TABLE 2: Polarizability of Fluoride Calculated with Explicit Solvent Molecules Added Either as Simple Point Charges (+0.41 au for the protons and −0.82 au for the oxygens) or Using a Supermolecule Approach[a]**

| | point charges | | | point charges + IEF-PCM | | |
|---|---|---|---|---|---|---|
| | aug | daug | HH | aug | daug | HH |
| HF | 5.18 | 7.86 | 7.88 | 5.40 | 8.36 | 8.36 |
| B3LYP | 6.16 | 10.49 | 10.62 | 6.47 | 11.36 | 11.42 |
| | supermolecule | | | supermolecule + IEF-PCM | | |
| | aug | daug | HH | aug | daug | HH |
| HF | 7.27 | 7.53 | | 8.30 | 9.61 | |
| B3LYP | 10.86 | 11.33 | | 13.94 | 14.36 | |

[a] Calculations have been performed using both the isolated system and embedding the cluster in the dielectric continuum.

replaces the oxygen and hydrogen atoms of the water molecules by point charges: in this case the only term that contributes the cluster polarizability is the fluorine ion.

In Table 2 we report the HF and B3LYP results obtained with these two approaches; to compute polarizability of the QM clusters (in the table indicated as "supermolecule"), we have used both aug-cc-PVDZ and daug-cc-pVDZ for $F^-$ but always in combination with aug-cc-pVDZ for the waters, while in the point charge approximation we have tested all three basis sets used in Table 1. For the values of the point charges we have used the popular SPCE water model,[28] which introduces a charge of −0.82 e for oxygen and +0.41 e for hydrogen. All these calculations have also been repeated by adding an external continuum so to include long-range (or bulk) effects.

The two alternative descriptions of the $F(H_2O)_6^-$ clusters give similar behaviors even if the absolute values of the resulting $\alpha$ are significantly different especially with the smallest basis set or when an external continuum is introduced. An analysis of these behaviors is not easy also because the polarizability derived from the "supermolecule" approach involves the assumption of additivity, which prevents quantitative comparisons. However, as here the main interest is to test alternative descriptions of the solvent, the most important analysis of the results of Table 2 is the comparison with what was previously found with a continuum-only description.

From Table 1 it has followed that with the uncorrelated method (HF) or standard basis set, fluoride polarizability increases passing from gas to solution, while with correlated methods and/or a large basis set (especially with that calibrated for polarizabilities) the opposite result is obtained. A similar behavior is found in the case of the "supermolecule" approach, while all the QM methods and all the basis sets give a decrease when point charges are used.

The results of the point-charge model can be explained in terms of the interactions of the electronic density of the ion with the closer shell of positive charges representing the protons and the farther shell of negative charges representing the oxygen atoms.

As the electrons are repelled by the negative charges and attracted by the positive ones, the net result is that the ion density will tend to remain inside the first positive shell and thus its polarizability is reduced with respect to the isolated ion. The picture is clearly demonstrated by the $\langle r^2 \rangle$ parameter (namely, the electronic spatial extent, ESE), which, for instance, at the B3LYP/HH level, goes from 18.1 au in the isolated ion to 16.2 au introducing the point charges.

It is interesting to make a comment on the similarities and the differences between the point charge model and the continuum-only model.

In the IEF-PCM model the presence of the negative ion induces a net positive apparent charge density on the cavity surface: the effect of this charge density will thus not be very different from that induced by the first shell of positive charges in the point-charge cluster, and, in fact, both models generate a parallel squeezing of the electronic density and a consequent decrease of the polarizability. The main difference between the point-charge model and the IEF-PCM is that in the IEF-PCM such an effect is counterbalanced by a strong opposite effect due to the normal electrostatic-induced enhancement of the solute polarizability: as a consequence, only with very diffused basis sets will the squeezing effect win and the net result of solvation is a decrease of the polarizability.

*3.1.2. Inclusion of Solute−Solvent Repulsion Effects*. A more accurate description of the solvent effect on these systems can be obtained by introducing, together with the electrostatic interaction, the solute−solvent repulsion. As shown in section 2.4, repulsion effects can be properly included in continuum models by means of an additional contribution to the effective Hamiltonian. We note that in the results shown in Tables 1 and 2 the repulsion effect was not included.

The inclusion of repulsion induces a further decrease of the polarizability with respect to the gas phase: at the B3LYP/HH level IEF-PCM+repulsion gives a polarizability of 13.83 au, while IEF-PCM without repulsion gives 15.16 au.

This preliminary investigation on fluoride can be summarized here in the following two points: (i) the B3LYP/HH level of calculation is the proper description to study the changes of the polarizability when going from gas to water solution, and (ii) the solvent can be properly described with a continuum method, but careful attention has to be paid to the inclusion of solute−solvent repulsive interactions.

To conclude this section, in Table 3 we report the results for all four halides at the selected (B3LYP/HH) level of theory for all three environments, namely, gas, electrostatic-only continuum solvent, and electrostatic-repulsive continuum solvent. We recall that in both continuum models the radii used for the spherical cavities of the halides are 1.47 Å for F, 1.75 Å for Cl, 1.85 Åfor Br, and 1.98 Å for I; all radii have been scaled by 1.2.[8]

The results in Table 3 show that for the electrostatic model the only halide that displays a significant reduction of the polarizability is fluoride (from 22.91 au to 15.16 au), while for $Cl^-$ this reduction is much less significant (less than 1 au). The other two halides exhibit an opposite behavior. On the other side, when repulsion is introduced, an increase in the polarizability is observed only for iodide and, with respect to the electrostatic-only model, all the anions display a smaller polarizability.

**TABLE 3: Polarizabilities of the Four Halide Anions at the B3LYP/HH Level**

| | $F^-$ | $Cl^-$ | $Br^-$ | $I^-$ |
|---|---|---|---|---|
| in vacuo | 22.91 | 42.71 | 55.19 | 75.48 |
| IEF (electrostatic) | 15.16 | 41.85 | 58.18 | 87.80 |
| IEF (el + rep) | 13.83 | 38.30 | 52.93 | 79.50 |

[a] The first row displays the in vacuo values, while in the second and in the third row the results for the solvated systems without repulsion and with repulsion are respectively collected. All values are in au.

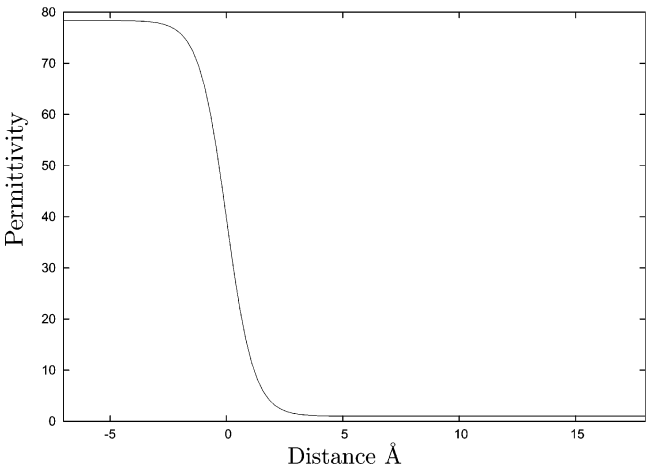


**Figure 2.** Permittivity profile $\epsilon(z)$ employed for interface calculations of halide static polarizabilities. The function is shown in the same range employed for interface calculations.

**3.2. Interface Calculations.** The results for the anion polarizability at the water/vacuum interface will be presented here. For each of the four halides, two series of calculations have been performed: one with the electrostatic model and the other with the electrostatic and repulsion model. For each series, the relevant properties of the anions have been computed varying the parameter $z$, which defines the position of the anion with respect to the interface profile, which for the solvent density is defined in eq 5 and for the dielectric permittivity is defined in eq 6.

Besides the polarizability $\alpha(z)$, which is our main goal here, we have also collected the solvation energy $G(z)$, the dipole moment $\mu(z)$, and the electronic spatial extent (ESE) $\langle r^2 \rangle(z)$.

The data will be discussed and interpreted comparing the results for the various quantities, the observed trends along the halide series, and comparing them to the available literature.

*3.2.1. Polarizability and Other Properties.* Following ref 10, in the present study we adopt a narrow interface. The corresponding profile of the permittivity is reported in Figure 2.

In Figure 3 the isotropic polarizability profiles of the four halides have been reported.

Starting from the bulk side (left side of each graph) we can see that the polarizability assumes nearly the bulk value in the range −4 to −6 Å depending on the size of the anion and on the inclusion of repulsion. This clearly demonstrates that the interface effect is short-ranged on the bulk side: on a molecular length scale, it corresponds to 2−3 solvation shells and it is

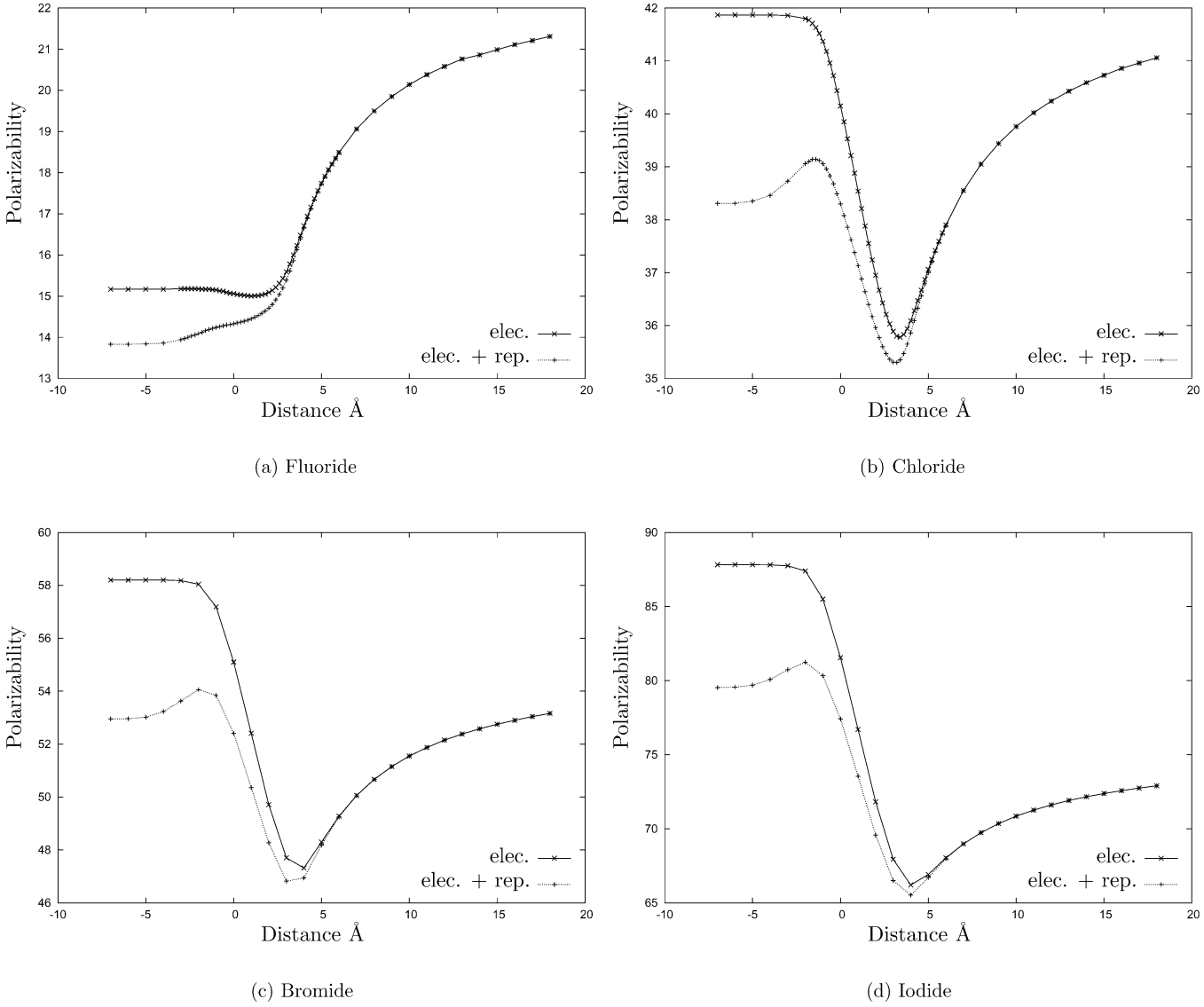


**Figure 3.** Polarizability profiles obtained for the four halides with the two employed methods, crossing the water/vacuum interface. Each graph refers to a different anion, ordered from the lighter to the heavier. In each graph we have reported the polarizability obtained with the electrostatics-only model (solid line with × marks) and with the electrostatics and repulsion model (dotted line with + marks). Distances are in Å and polarizabilities in au.

consistent with the common knowledge that three solvation shells are enough to provide a bulk-like behavior.

On the vacuum side of the graph, the picture is opposite: the interface effect is extremely long-ranged and, in fact, none of the four anions reaches the gas-phase value of the polarizability at 18 Å. [We have observed that to reach polarizabilities comparable with the gas-phase values, one has to go as far as 100 Å from the interface. These points have not been included in the reported plots for practical reasons.]

We proceed now to analyze the region of space between −5 and 10 Å.

First, a clear distinction between fluoride and the three heavier halides can be drawn: while all three heavy halides display a clear minimum for the polarizability in the range of $z = 2-3$ Å, fluoride shows just a very small minimum. When repulsion is introduced, the minimum in the fluoride profile disappears, whereas for the three other halides it becomes more pronounced. Another interesting effect arising when repulsion is employed is the appearance of a maximum around −2 Å. Once again, for fluoride no maximum is observed but only an inflection in the curve. The presence of this maximum can probably be explained as follows: in bulk solution repulsion has the effect of compressing the electronic density, thus reducing the polarizability. When the interface is approached, this effect is reduced; on the other hand, the electrostatic contribution, being subject to a saturation effect, is almost as in bulk solution. The net result is the maximum in the polarizability profile. The successive minimum is instead electrostatic in nature since it is already present when only electrostatic solvation is used: this assertion will be confirmed by the analysis of dipole moments (vide infra).

For monatomic species in bulk solution and vacuum, spherical symmetry applies, whereas the interfacial environment induces a symmetry breaking, reducing the symmetry to $C_{\infty v}$. The most evident consequence is the ion polarization and the appearance of a dipole moment along the direction perpendicular to the plane. Figure 4 shows the resulting dipoles for the four anions.

Comparing the two graphs it is evident that dipole moments are not very sensitive to the presence of repulsion: the two sets of curves—with and without repulsion—look fairly similar. Moreover, comparing Figure 4 with Figure 3 we can confirm the electrostatic nature of the minimum in the polarizability plots, since it closely corresponds to the maximum of the dipole

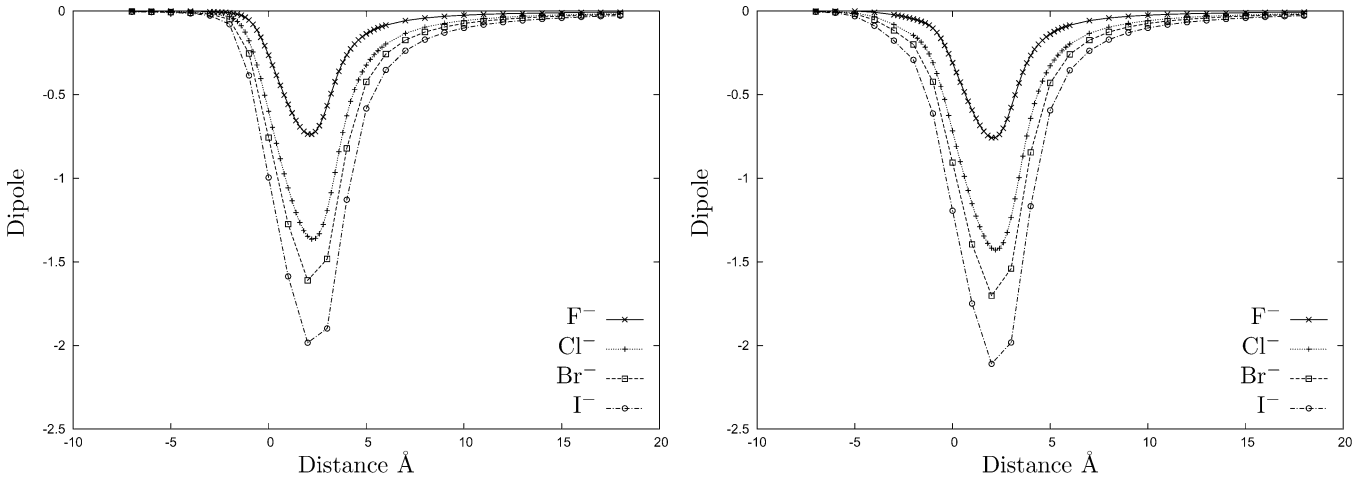


**Figure 4.** Dipole moments of the four halides crossing the water/vacuum interface. On the left side electrostatic model results are collected, whereas on the right side electrostatics and repulsion results are shown. Distances are in Å, and dipoles are in Debye.

moment. The reason for such coincidence is clear. The dipole moment produced by the polarization of the electronic cloud along the *z* direction results also in an enhancement of its "stiffness". Therefore it reduces its tendency to polarize further; in other words, it lowers the polarizability.

Another consequence of the symmetry breaking is that the polarizability tensor, though still diagonal in the selected reference frame, can be decomposed in two parallel ($\alpha_{xx}$ and $\alpha_{yy}$) and a perpendicular component ($\alpha_{zz}$). In Figure 5, parallel ($\parallel$) and perpendicular ($\perp$) components have been displayed for both the purely electrostatic and the electrostatics and repulsion model. To allow for a comparison along the series of the four halides, the results are here reported as relative variations with respect to the in vacuo value: $\Delta\alpha_X(z) = (\alpha_X(z) - \alpha_X^{vac})/\alpha_X^{vac}$ with $X = \parallel$ or $\perp$.

Apart from the features that are in common with the isotropic polarizability, we would like to draw attention to the small maximum in the perpendicular component of the polarizability that is present in both electrostatic-only and electrostatic + repulsion models.

To investigate the reason for such peculiar behavior, we have first tried to interpret it in light of other properties, like what has been done comparing the dipole with the isotropic polarizability. A property that generally well correlates with the polarizability is the average value of $r^2$ over the electronic distribution, namely, the previously defined ESE, $\langle r^2 \rangle$. The ESE relative variations with respect to the in vacuo value are reported in Figure 6.

As expected, in all cases, $\Delta\langle r^2 \rangle$ is negative, or in other words, the electronic cloud of the ions is "compressed" by the solvent. This is particularly evident in fluoride, for which such "compression" is around 8−10% (depending whether the model contains repulsion or not). This is a remarkable result considering that fluoride is the smallest and the stiffest of the four halides. The other three electronic densities are much less affected, and the corresponding compressions range from 3.5% to 6.5% depending on the ion and the inclusion of repulsion.

The analysis in terms of the ESE, however, does not explain the presence of minima and maxima in the polarizability since its trend is always monotonic.

As a further analysis, we have thus performed a series of calculations of the *intrinsic polarizability* of fluoride and chloride.

We recall that the *intrinsic polarizability* is the polarizability calculated without including the solvent terms in the response calculation. Referring to the theory presented in section 2.5, the intrinsic polarizability is calculated without the explicit solvent contributions defined in eq 22 but still keeping the solvent effect in the SCF procedure to compute the wave function.

The results for the two components (parallel and perpendicular) of the intrinsic polarizability of the two halides are reported in Figure 7.

The most evident feature here is the substantial difference with respect to the corresponding components of the total (as opposed to intrinsic) polarizability (see Figure 5). While the components of the total polarizability present a structure of maxima and minima, those of the intrinsic polarizability are almost monotonic, except for a small minimum in the perpendicular component of the electrostatic model. On the other hand, the intrinsic polarizability correlates very well with the ESE: for both anions these two properties increase passing from solution to gas phase. This consideration led us to the conclusion that the structure observed at the interface for the total polarizability (see Figure 5) and the net increase of the total polarizability of iodide from the gas phase to solution (see Table 3) are due to the combination of the two solvent effects, namely, that on the wave function and that in the response equations. It is thus of fundamental importance to introduce solvent effects in the calculation of the property: this can be achieved by correctly generalizing the response theory to molecular systems in the presence of the solvent reaction field as shown in eqs 20−22.

As a final analysis, it is interesting to compare the results for the polarizability with the energy profiles that are displayed in Figure 8.

From the solvation energy profiles it can be seen that electrostatics alone gives rise to a monotonic curve passing from bulk to vacuum. On the other hand, when repulsion is added, the resulting solvation energy profiles display a clear minimum. This minimum is located almost in the same position as the maximum of the polarizability for the heavy halides, whereas for fluoride it corresponds to the small inflection at −2 Å. We can compare the obtained minima for the solvation energy ($F^-$: −0.1 kcal/mol, $Cl^-$: −0.7, $Br^-$: −0.9 kcal/mol, $I^-$: −1.4 kcal/mol) with the results from Dang[29] ($Cl^-$: no minimum, $Br^-$:

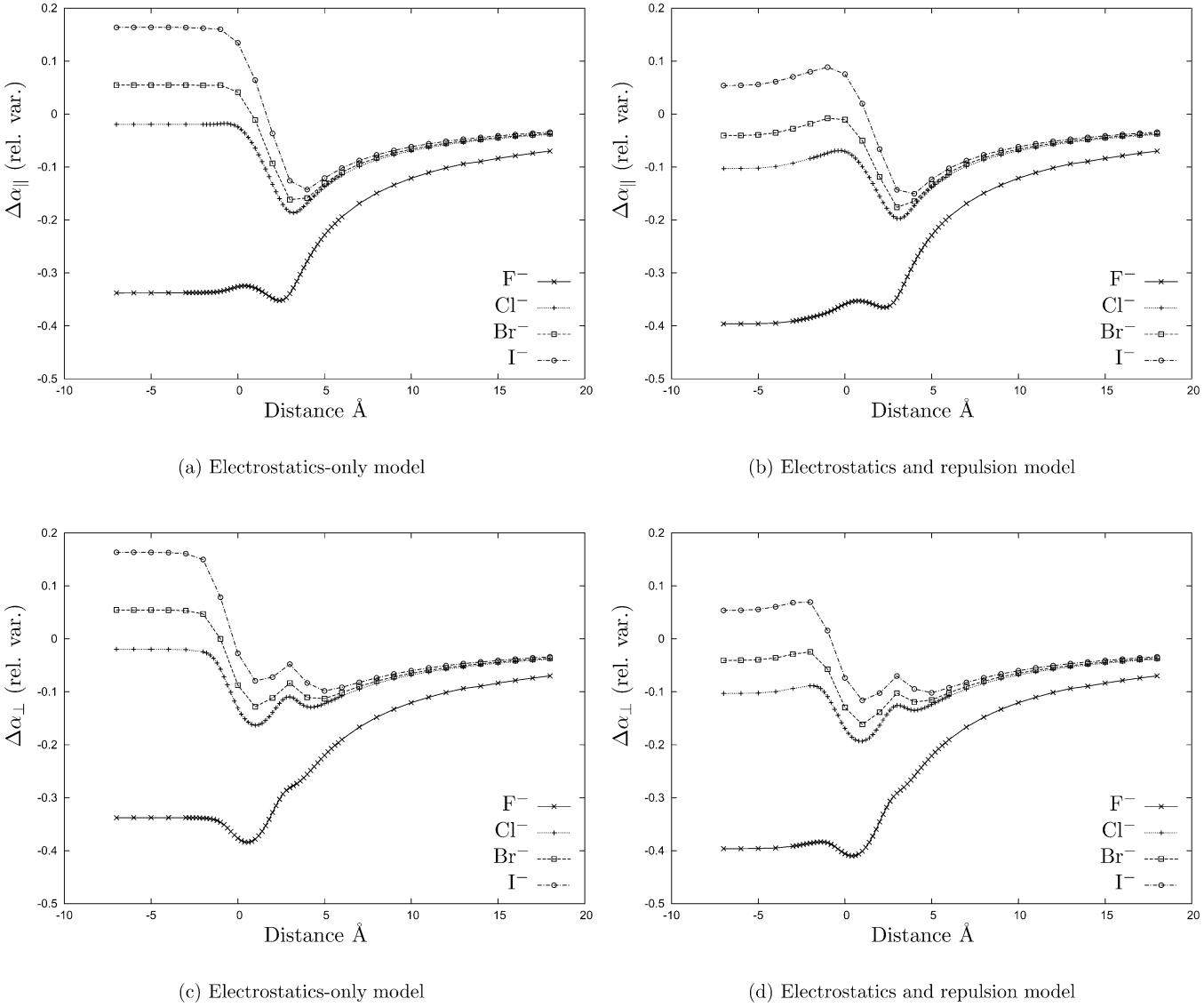


**Figure 5.** Parallel (upper graphs) and perpendicular (lower graphs) components of the polarizability tensor of the four halides crossing the water/vacuum interface. On the left side electrostatic model results are collected, whereas on the right side electrostatics and repulsion results are shown. Distances are in Å, and polarizabilities are shown as relative variations with respect to the vacuum values.

−0.9 kcal/mol, $I^-$: −1.5 kcal/mol). Very good agreement is obtained for the heavier ions, while for chloride the two results are qualitatively different. Our findings are, however, in qualitative agreement with Jungwirth and Tobias,[4] who observed a surface preference for chloride as well.

From these results it seems that the surfactant behavior of the heavy halides is not uniquely determined by their polarizability (i.e., if we allow them to polarize), but more probably by a combination of effects of electrostatic and repulsive nature. We have to stress, however, that these results are preliminary and that important solute−solvent interactions have not been included in the model. In particular, dispersive effects between solute and solvent are here completely neglected, exactly as possible specific effects arising at the liquid/gas surface between the ion and the solvent molecules, which could give rise to local modifications of the solvent properties. In any case, it is interesting to note that continuum models can indeed reproduce the results observed with discrete simulations.

## 4. Concluding Remarks

In this work we have focused on the study of the static polarizability of halides (fluoride, chloride, bromide, and iodide) at the water/air interface. This property has then been connected to other relevant quantities such as the free energy profiles and the dipole moment.

The obtained profiles of the polarizability $\alpha(z)$ as a smooth function of the distance of the anion from the interface show a nonobvious structure of minima and maxima both in the isotropic and in the parallel and perpendicular components. This structure has been well correlated to the anisotropy of the environment at the interface by comparing the polarizability with other molecular properties.

Another result of the present study concerns the role of the various physical interactions that concur in determining the behavior of the heavier halides. As it has been said, previous MD works attributed to the polarizability the role of yielding the halides surface preference. Here, the comparison of two different continuum models (electrostatic-only and electrostatic + repulsion) seems to indicate that there exists a more complex situation in which polarization and repulsion effects combine to give the observed interfacial preference of the heavier halides.

However, it has to be remarked that the present one is not a study on the surfactant behavior of halides but an attempt to exploit continuum models to accurately compute a property,

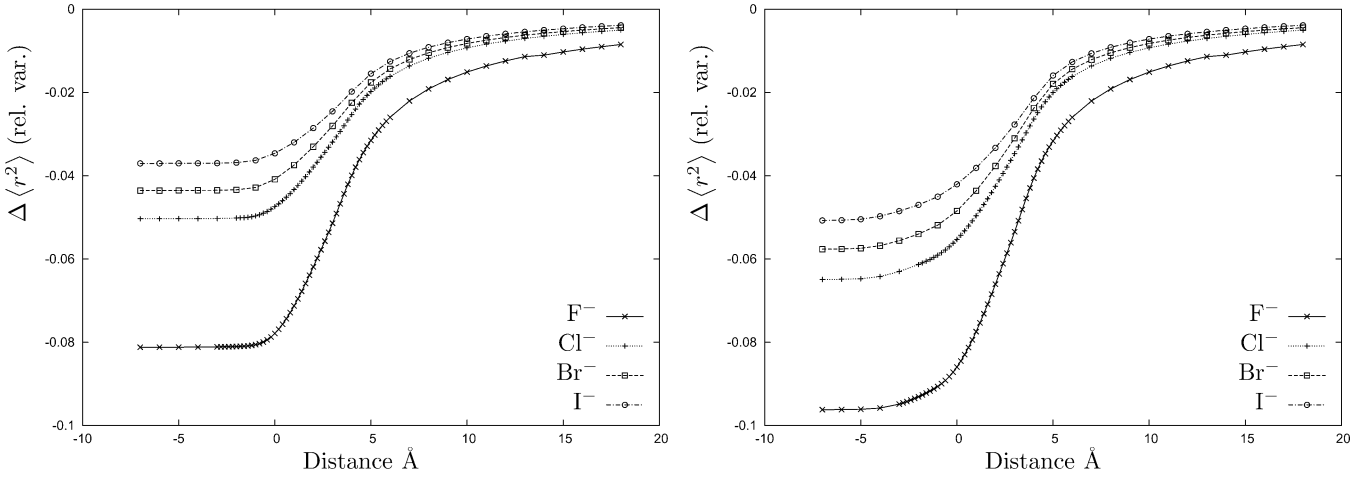


(a) Electrostatics-only model (b) Electrostatics and repulsion model

**Figure 6.** Electronic spatial extent of the electronic cloud of the four halides crossing the water/vacuum interface. Distances are in Å, and ESEs are reported as relative variations with respect to the vacuum values.

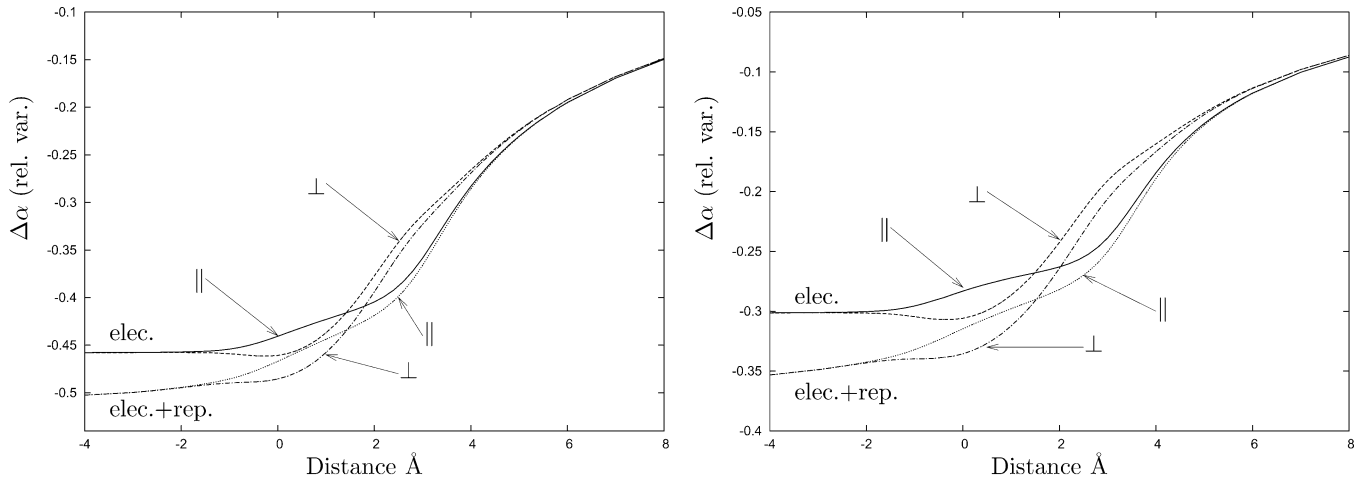


(a) Fluoride intrinsic polarizability components (b) Chloride intrinsic polarizability components

**Figure 7.** Parallel and perpendicular components of the intrinsic polarizability tensor for fluoride (left side) and chloride (right side). Both the electrostatics-only model and electrostatics and repulsion model are shown. Distances are in Å, and polarizabilities are shown as relative variations with respect to the vacuum values.

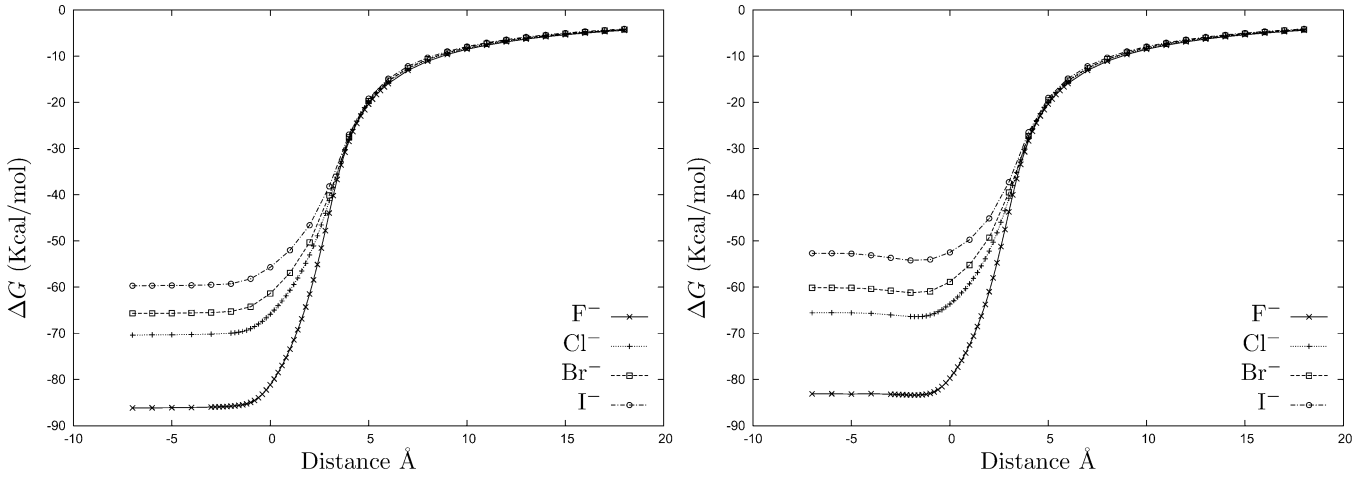


(a) Electrostatics-only model (b) Electrostatics and repulsion model

**Figure 8.** Solvation energy profiles of the four halides. On the left side the profiles obtained with the electrostatic-only model are shown, while on the right side the profiles obtained with the electrostatics and repulsion model are shown. Distances are in Å, and energies are in kcal/mol.

the polarizability, that surely plays a key role in such phenomenon. The good correlation we have found between the polarizability and the free energy profiles indeed confirms the importance that this property has in the behavior of halides at the liquid/gas interfaces. However, other and more detailed calculations should be performed to achieve a completely reliable picture of the energetic profiles. These calculations should not only include all solute−solvent interactions (for example, dispersion effects that have been neglected here) but also take into account more specific interface effects such as the orientational polarization of the solvent molecules around the anions and the surface corrugation.

On the other hand, the present work represents one of the most accurate quantum-mechanical studies of the polarizabilities of anions at interfaces; for the first time, in fact, a coherent approach has been used to describe the molecular property in the bulk solution, at the interface and in the gas phase. An accurate version of electrostatic continuum models (the well-known IEF-PCM) has been used and supplemented with a model for including repulsion effects in the quantum-mechanical description of the solute; both these models have then been generalized so to account for the presence of the interface still maintaining the same level of accuracy.

Obviously, in the present description of polarizabilities our model still lacks some aspects of the solute−solvent interactions. In particular, it would be interesting to check the contribution of dispersion effects on this property. Not much has been done in the past on the role of dispersion in the solvent-induced effects on molecular properties and, in particular, on polarizabilities. As far as concerns continuum approaches, there is a previous quantum mechanical study on nonelectrostatic effects on static polarizabilities of neutral molecules in bulk solution that showed a substantial predominance of the repulsion contribution with respect to the dispersion contribution.[30] This result makes us confident that the present analysis, carried out neglecting the dispersive interaction, is substantially correct, even if we have clearly in mind that there are important differences between that work and the present one, and that there is the chance that dispersion interactions could be more significant at the interfacial region, where there is more free volume and thus repulsion is less important.

**Acknowledgment.** Dr. C. Hattig is kindly acknowledged for having provided the basis set functions.

## References and Notes

(1) Hu, J. H.; Shi, Q.; Davidovits, P.; Worsnop, D. R.; Zahniser, M. S.; Kolb, C. E. *J. Phys. Chem.* **1995**, *99* (21), 8768.
(2) Onsager, L. *Chem. Rev.* **1933**, *5*, 73.
(3) Onsager, L.; Samaras, N. N. T. *J. Chem. Phys.* **1934**, *2*, 528.
(4) Jungwirth, P.; Tobias, D. J. *J. Phys. Chem. B* **2002**, *106* (25), 6361.
(5) Morita, A.; Kato, S. *J. Chem. Phys.* **1999**, *110* (24), 11987.
(6) Mennucci, B.; Cammi, R.; Tomasi, J. *Int. J. Quantum Chem.* **1999**, *75*, 767.
(7) Miertus, S.; Scrocco, E.; Tomasi, J. *Chem. Phys.* **1981**, *55*, 117.
(8) Tomasi, J.; Persico, M. *Chem. Rev.* **1994**, *94*, 2027.
(9) Frediani, L.; Pomelli, C. S.; Tomasi, J. *Phys. Chem. Chem. Phys.* **2000**, *2*, 4876.
(10) Frediani, L.; Cammi, R.; Corni, S.; Tomasi, J. *J. Chem. Phys.* **2004**, *120* (8), 3893.
(11) Cancès, E.; Mennucci, B.; Tomasi, J. *J. Chem. Phys.* **1997**, *107* (8), 3032.
(12) Cancès, E.; Mennucci, B. *J. Math. Chem.* **1998**, *23*, 309.
(13) Mennucci, B.; Cammi, R.; Tomasi, J. *J. Chem. Phys.* **1998**, *109* (7), 2798.
(14) Corni, S.; Tomasi, J. *J. Chem. Phys.* **2001**, *114*, 3739.
(15) Corni, S.; Tomasi, J. *J. Chem. Phys.* **2002**, *117*, 7266.
(16) Michael, D.; Benjamin, I. *J. Phys. Chem. B* **1998**, *102*, 5145.
(17) Goujon, F.; Malfreyt, P.; Boutin, A.; Fuchs, A. H. *J. Chem. Phys.* **2002**, *116* (18), 8106.
(18) Lie, G. C.; Grigoras, S.; Dang, L. X.; Yang, D.-Y.; McLean, A. D. *J. Chem. Phys.* **1993**, *99* (5), 3933.
(19) Taylor, R. S.; Dang, L. X.; Garrett, B. G. *J. Phys. Chem.* **1996**, *100*, 11720.
(20) Dang, L. X.; Chang, T.-M. *J. Chem. Phys.* **1997**, *106* (19), 8149.
(21) Amovilli, C.; Mennucci, B. *J. Phys. Chem. B* **1997**, *101* (6), 1051.
(22) Cammi, R.; Cossi, M.; Mennucci, B.; Tomasi, J. *J. Chem. Phys.* **1996**, *105* (23), 10556.
(23) Cammi, R.; Cossi, M.; Tomasi, J. *J. Chem. Phys.* **1996**, *104* (12), 4611.
(24) Hattig, C.; Hess, B. A. *J. Chem. Phys.* **1998**, *108*, 3863.
(25) Woon, D. E.; Dunning, T. H. *J. Chem. Phys.* **1994**, *100*, 2975.
(26) Huzinaga, S.; Klobukowski, M. *Chem. Phys. Lett.* **1993**, *212*, 260.
(27) Jungwirth, P.; Tobias, D. J. *J. Phys. Chem. A* **2002**, *106*, 379.
(28) Berendsen, H. J. C.; Grigera, J. R.; Straatsma, T. P. *J. Phys. Chem.* **1987**, *91*, 6269.
(29) Dang, L. X. *J. Phys. Chem. B* **2002**, *106*, 10388.
(30) Mennucci, B.; Amovilli, C.; Tomasi, J. *Chem. Phys. Lett.* **1998**, *286*, 221.